Original Article

Institution of MECHANICAL ENGINEERS
Journal of MATERIALS: DESIGN AND APPLICATIONS

Proc IMechE Part L:
J Materials: Design and Applications
0(0) 1–13

DOI: 10.1177/1464420713507411
pil.sagepub.com
SAGE

Investigation of scaling effects on fiber metal laminates under tensile and flexural loading

Masoud Haghi Kashani[1], Mojtaba Sadighi[1], Melika Mohammadkhah[1] and Hamid Shahsavari Alavijeh[2]

Abstract

In this study, scaling effects on fiber metal laminates under tensile and three-point bending tests were investigated numerically and experimentally. The fiber metal laminate specimens were made of aluminum 1050 and unidirectional glass–epoxy. Two scaled sizes of specimens were prepared based on $[Al_n, 0^\circ_n/90^\circ_n]_s$. Some specified mechanical properties of these samples were investigated and results showed that fiber metal laminates obey scaling law under quasi-static loading. Explicit finite element code LS-DYNA was utilized for numerical simulation. After validating numerical simulation with experiments, scaling law was studied numerically for four different sample sizes. Finite element analysis demonstrated that scaling law is valid for fiber metal laminates. In final part, hole size effect in FML specimen was investigated numerically.

Keywords

Scaling effect, fiber metal laminates, tensile loading, three-point bending

Date received: 3 February 2013; accepted: 14 August 2013

Introduction

Fiber metal laminates (FMLs) represent an excellent type of material made from a combination of a metal and a fiber-reinforced composite. Currently, FMLs such as GLARE (GLAss-REinforced aluminium laminate) are being used in quite a few industries especially aircraft and aerospace because this type of material shows great fatigue and impact resistance as opposed to either monolithic aluminum or fiber-reinforced composite materials.[1–3]

Therefore, knowing the behavior of this material under different expected and unexpected loads is a very important issue, but investigating the behavior of engineering components with real size under different experiments is expensive and a time-consuming process. This problem leads to present scaling rule in order to predict the behavior of real parts by using the result of laboratory specimens.

Although a few studies were performed about the validation of scaling law in FMLs, many studies have been carried out in order to understand scaling effects in composite structures under different loading conditions. This fact is because composite materials play a key role in quite a few industries, which has caused the scientists to pay more attention to this subject. As an illustration, Morton[4] used Buckingham theorem to investigate scaling effects in the low velocity impact response of carbon-fiber composites. He showed that the impact duration scaled as the scale factor and the impact force as the square of the scale factor. Sutherland and Guedes Soares[5] and Viot et al.[6] also used dimensionless governing parameters to predict composite structures behavior and verify the analytical results with experiments using different scale models. Christoforou et al.[7] established scaling rules for the impact response of different structures such as rods, beams, and plates. Qian et al.[8] and Swanson[9] investigated scaling effects in the impact damage of fiber-reinforced composites. They tested five geometrically scaled sizes of carbon–epoxy plate under low and high velocity impact to investigate scaling effects below and above the damage threshold energy. Kellas et al.[10,11] used the Buckingham theorem to research about scaling effects in the tensile and flexural properties of a carbon–epoxy composite. Wisnom[12] investigated scaling rules under four-point bending and in

[1]Department of Mechanical Engineering, Amirkabir University of Technology, Tehran, Iran
[2]Department of Mechanical Engineering, Sharif University of Technology, Tehran, Iran

Corresponding author:
Mojtaba Sadighi, Department of Mechanical Engineering, Amirkabir University of Technology, P.O. Box 15875-4413, Tehran, Iran.
Email: mojtaba@aut.ac.ir

buckling and found that scaled carbon fiber–epoxy specimens have a size dependency.

Carrillo and Cantwell[13] undertook a study of scaling effects in new FMLs. The investigation focused on the feasibility of scaling law to predict the behavior of full-scale specimen—the biggest specimen among all studied specimens. They performed tensile tests on the FML specimens which were scaled according to the three approaches including 1D scaling (the thickness of specimens is scaled), 2D scaling (the in-plane dimensions are scaled), and 3D scaling (all the dimensions are scaled). The results showed that there were little differences between ultimate stresses of different size-scaled specimens. However, the elastic modulus of the FMLs was approximately constant over different sizes of specimens. In another research, they[14] focused on evaluating the possibility of using scale model tests for predicting the full scale low velocity impact response of FMLs based on $[Al, 0^\circ/90^\circ]_{ns}$ and $[Al_n, 0^\circ/90^\circ{}_n]_s$ configurations. These two configurations were used to scale four different sample sizes. They showed that the deformation modes and failure mechanisms were similar in all four scaled sizes. Other parameters such as the maximum impact force and the time to maximum load showed little sensitivity to scale size. McKown et al.[15] looked into scaling effects in a novel FML—manufactured from a self-reinforced polypropylene fiber/polypropylene matrix composite and a 2024-O aluminum alloy—through a series of tensile, four-point bending, and low velocity impact tests. They showed that no significant scaling effects on tensile and flexural properties were observed in the mechanical response of the laminates. Also, an examination of the failed samples subjected under tensile and four-point bending tests indicated that the fracture mode was not changed with increase in scale size. Additionally, he and his research group found out that such response parameters as the target deflection, the impact force, and the damage threshold energy obey the scaling law.

The notched strength of composite materials has been investigated enormously over the past 30 years because of its importance to designers and manufacturers. One of the widely researched event related to notched strength is the ''hole size effect,'' whereby the strength of a laminate decreases with increasing hole diameter for a constant stress concentration across the width of a specimen.[16] Early work in the field of scaling of notched composites focused on developing semiempirical analytical models for the prediction of notched strength. Some studies have shown that in notched specimens scaling is accompanied by the well-known ''hole size effect'' whereby strength decreases with increasing hole size.[17–19] An assessment of scaled tests on unnotched and open-hole tension and compression specimens was carried out by Winsom and Hallett.[20] Carbon-fiber epoxy specimens have been tested using two different scaling techniques: sublaminate-level $[45/90/-45/0]_{ns}$ and ply-level scaling $[45_n/90_n/-45_n/0_n]_s$, with different thickness and in-plane dimensions. They compared failure mechanisms and scaling behavior between tension and compression and presented models that predict the observed size effects. Green et al.[21] designed an extensive experimental program to investigate the effects of scaling on the strength of notched composites. The most important variables were identified as notch size and laminate thickness. In 3D scaled cases, strength decreased as specimen size increased. Another investigation of the effect of size on the tensile strength of composite laminates containing circular hole has been conducted by Hallett et al.[22] They showed that a large difference both in failure stress and mechanism due to changes in test configuration is impressed by size effect on the tensile strength of composite laminates containing circular hole. Winsom and Hallett[23] performed several series of open-hole tension tests on quasi-isotropic IM7/8552 carbon fiber–epoxy laminates with the same stacking sequence but different ply block thicknesses and numbers of sublaminates. They examined the role of delamination in strength, failure mechanism, and hole size effect in quasi-isotropic laminates.

According to the literature, the focus on the evaluation of scaling law was experimental, and no numerical studies were reported about the FMLs. As a result, the goal of the present paper is to investigate the validation of scaling law in FMLs numerically as well as experimentally under tensile and three-point bending tests. In addition, the comparison between numerical and experimental results has been made in this study. Inasmuch as the studies related to the investigation of notched strength of FMLs were limited, the hole size effect in FML specimen was investigated numerically in this study, as well.

Experimental study

In this study, tensile and three-point bending tests were performed on FMLs which were made of aluminum 1050 and unidirectional glass–epoxy. FML specimens were prepared by hand-layup technique in the room temperature. The P2 ETCH method[24] was utilized for the surface treatment of aluminum sheets in order to better bond between the metal and composite layers. Also, the specimens were subjected to the pressure of 200 MPa for 24 h.

In order to achieve more accurate numerical results, the correct value of mechanical properties was required. Thus, the first experiments were conducted on the aluminum sheets and glass epoxy laminates under tensile loading to find the mechanical properties of them. All of these tests were done according to ASTM D3039. The mechanical properties were obtained from these experimental data tabulated in Tables 1 and 2.

For investigating the scaling rule, two methods are generally used which are known as sublaminate-level

Table 1. Mechanical properties of aluminum sheets.

Property	Unit	Value
Young's modulus	GPa	68
Yield stress	MPa	91
Density	kg/m^3	2.69e3
Poisson's ratio	–	0.33
Maximum plastic strain	–	18%
Ultimate stress	MPa	134

Table 2. Mechanical properties of glass–epoxy plies.

Property	Unit	Value
E_{11}	GPa	41
E_{22} and E_{33}	GPa	9.3
G	GPa	4.2
Density	kg/m^3	1.93e3
Poisson ratio	–	0.3
Shear strength	MPa	110
σ_{11}^{C}	MPa	436
σ_{22}^{C} and σ_{22}^{C}	MPa	180
σ_{11}^{t}	MPa	870
σ_{22}^{t} and σ_{33}^{t}	MPa	133

and ply-level scaling.[14] In sublaminate-level method, the thickness of laminate increases by scaling the thickness of each plies whereas in the second approach, the thickness of laminate increases by repeating the sublaminate block several times. In this paper, sublaminate-level scaling was utilized, so two specimen sizes of FMLs with different values of n were investigated experimentally. n is the scale factor derived from the characteristic geometrical length ($n = 1$ is defined as the full-scale size). In experimental study, n has two values: ½ and 1. So, the thickness of aluminum layers which were used in this study was 0.4 and 0.8 mm, as well as the thickness of composite layers was 0.45 and 0.9 mm. Also all of the specimens are based on the following stacking sequences:

$$\left[\mathrm{A1}_n, \frac{0^\circ_n}{90^\circ_n}\right]_s$$

To achieve more accuracy, three samples of each specimen were tested and the mean value of the obtained data was considered as the final result.

Tensile test on FMLs

In this part of the study, FML specimens based on the two scaled sizes illustrated in Figure 1 were tested in tension that the dimensions of specimens were chosen according to ASTM D3039. The thickness of specimens measured 2.6 and 5.2 mm for smaller specimen ($n = 1/2$) and bigger one ($n = 1$). INSTRON 8502 hydraulic machine equipped with 250 kN load cell was used in this project for uniaxial tension tests. Also the strain rate in all tests was $0.01\,\mathrm{min}^{\uparrow}(-1)$ according to ASTM D3039.

Three-point bending tests

Three-point bending test was another kind of experiment which was conducted to find the scaling effects on FMLs. Two scaled sizes of FMLs specimen were used in these experiments whose dimensions were selected by using ASTM D790 as shown in Figure 2. The width of specimens measured 12.7 and 25.4 mm for smaller specimen ($n = 1/2$) and bigger one ($n = 1$), respectively. Also, the thickness of specimens used in tensile and three-point bending tests is the same.

Finite element modeling

Finite element methods offer advantages over analytical techniques. Finite element methods can be used to model many types of geometries and boundary conditions by changing the input parameters. Furthermore, finite element models can be scaled up to simulate entire structures. Some commercial finite element codes, such as LS-DYNA,[25] were used to develop numerical simulations of the FMLs under low and high velocity impacts. In this research, FMLs under tensile loading and three-point bending are modeled with LS-DYNA. Scaling law was investigated numerically for four different sample sizes ($n = 1/4$, 1/2, 3/4, and 1).

Modeling FMLs under tensile loading

FMLs contain aluminum and fiber composite layers. All the layers were modeled with solid element instead of shell element to ensure better compatibility between numerical and experimental results.[26,27] Aluminum has elastic–plastic behavior, so elastic-linear plastic material (type 24) was utilized for aluminum layers. Mechanical properties for this material were defined according to the result of aluminum specimen under tensile loading which was presented in Table 1. Also, the material which is selected to present behavior of glass fiber epoxy layers was "MAT_COMPOSITE_SOLID_FAILURE_MODEL" (type 59)[26] and mechanical properties for this material were defined according to Table 2. Layers in FMLs stick together and when delamination occurs, these layers are separated, so tiebreak contact was used to identify contact between plies. In the tensile test, one of the grips is constant and the other grip moves with constant rate; therefore in numerical modeling, one side of specimen is constrained in all of degrees and other side moves by using "BOUNDARY_PRESCRIBED_MOTION_SET" command in code. Also "DATABASE_NODAL_FORCE_GROUP" command was used to obtain load at each displacement. In order to diminish the

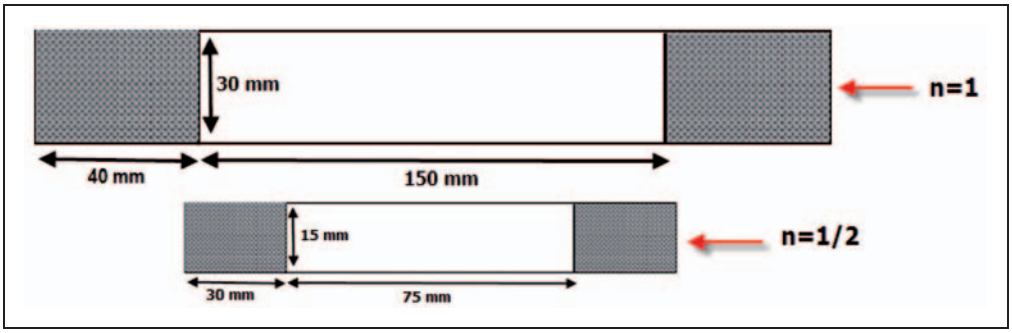

Figure 1. FML specimens' geometry under tensile loading.

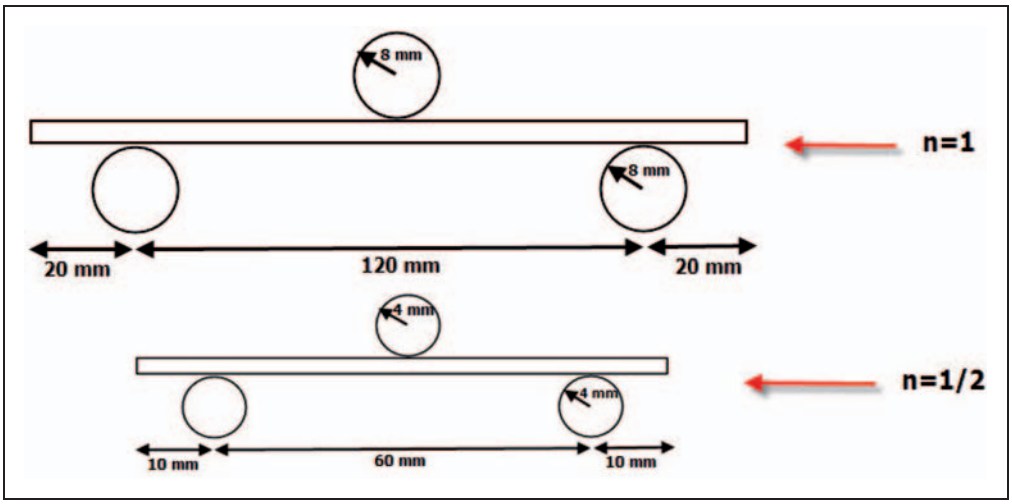

Figure 2. FML specimens' geometry under three-point bending.

Table 3. Obtained mechanical properties for tested FML specimens.

	$n = 1/2$	$n = 1$	Difference (%)
Elastic modulus (Gpa)	46.7 ($_{\downarrow} -^{\uparrow} +$)0.8)	44.9 ($_{\downarrow} -^{\uparrow} +$)1.1)	4
Yield stress (MPa)	94.4 ($_{\downarrow} -^{\uparrow} +$)1.2)	97.1 ($_{\downarrow} -^{\uparrow} +$)0.7)	3
Ultimate stress (MPa)	314 ($_{\downarrow} -^{\uparrow} +$)2.5)	303 ($_{\downarrow} -^{\uparrow} +$)3.6)	3.7
Maximum strain (%)	1.906 ($_{\downarrow} -^{\uparrow} +$)0.018)	1.760 ($_{\downarrow} -^{\uparrow} +$)0.023)	8.5

Table 4. Experimental and numerical tensile results for smaller FML specimen.

	Experimental	Numerical	Error (%)
Ultimate stress (MPa)	314 ($_{\downarrow} -^{\uparrow} +$)2.5)	338	9
Maximum strain (%)	1.906 ($_{\downarrow} -^{\uparrow} +$)0.018)	1.84	3.6

computation time in simulation of the quasi-static loading condition, mass scaling is applied.[28]

Modeling FML under three-point bending test

Modeling three-point bending contains two parts: FML specimen and loading nose. FML sample was modeled by using a method which was presented in tensile modeling; also sample was modeled according to the dimensions which are tabulated in Table 4. Loading nose was modeled with shell elements instead of solid elements to reduce run time. In order to improve the compatibility between numerical and experimental results, loading nose was assumed rigid,

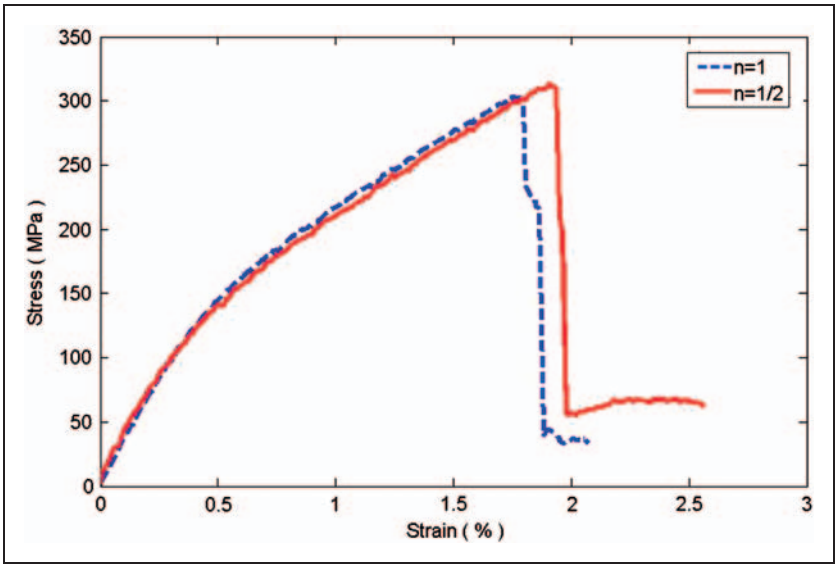

Figure 3. Comparison of experimental stress–strain curves for two scaled sizes of FMLs under tensile loading.

so MAT_RIGID (type 20) was used for this part. For defining the velocity of loading nose, "BOUNDARY_PRESCRIBED_MOTION_RIGID" command was utilized for loading nose with constant rate according to the speed in experiments. In this modeling, two contact models were applied where one of them was tiebreak contact which was used to identify contact between layers of FML similar to tensile modeling. Contact between loading nose and specimen was another contact which was applied by using automatic surface-to-surface contact. In order to diminish the computation time in simulation of the quasi-static loading condition, mass scaling is applied as well.

Results and discussion

This section presents and discusses the numerical and experimental results related to the scaling effect of FMLs through tensile and three-point bending tests in order to show that the response of FMLs under tensile and three-point bending test obeys scaling rules. Also, the compatibility between the numerical and experimental results has been evaluated in this section. In the last part of this section, scaling effects on FML specimen with an open hole are discussed.

Tensile results

Two scaled sizes of FMLs were tested and stress–strain curves which were obtained from experiments are shown in Figure 3. According to this figure, similar trend of both curves is seen in elastic, plastic, and rupture parts. Consequently, scaling has no effect on general tensile behaviors of FMLs. It was observed that failure modes are similar in both cases, and these failure modes included fiber breakage, delamination between composite layers, debonding between metal and composite layers, and aluminum fracture (see Figure 4). In both types of specimens, composite plies failed before the aluminum layers, also fracture in all cases occurred at 90° to the load direction.

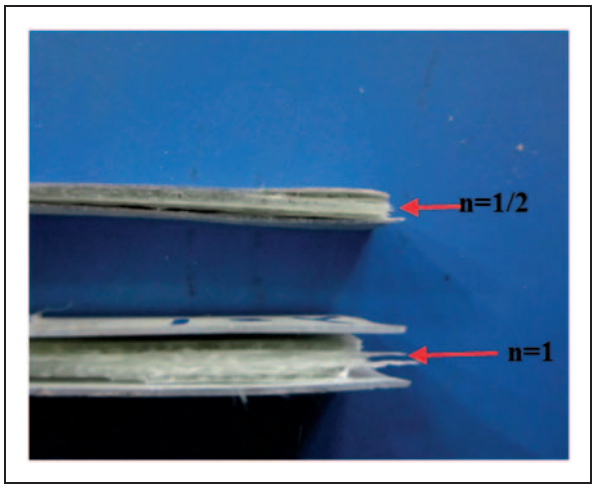

Figure 4. Two different scaled sizes of FML specimens after tensile test.

Figure 3 shows that both curves are very close together in elastic and plastic parts, but by approaching the rupture part, curves deviate from each other. It can be concluded that FMLs obey scaling rules in elastic and the beginning of plastic part, but it cannot be definitely said that the scaling law is valid for FMLs near rupture point under tensile loading. In order to study the effects of scaling on the structure behavior in detail, some specified mechanical properties have been investigated. Elastic modulus, maximum strain, yield, and ultimate stress of two scaled sizes were tabulated in Table 3. In order for difference

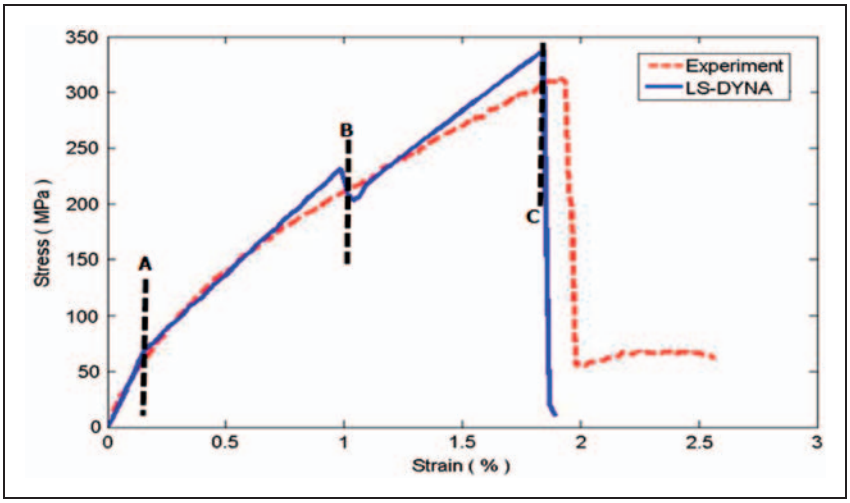

Figure 5. Comparison of numerical and experimental stress–strain curves of half scaled FML specimen under tensile loading.

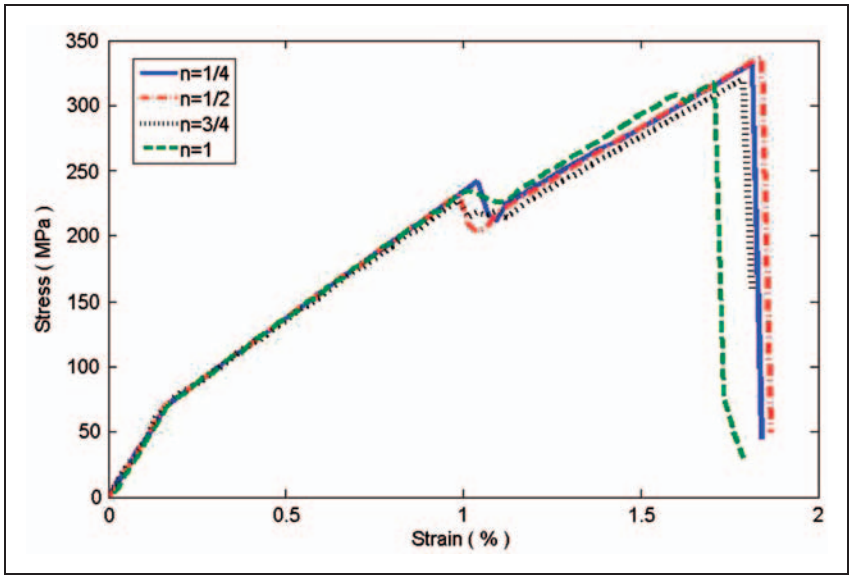

Figure 6. Comparison of normalized stress–strain curves for different scaled sizes of FMLs (numerical results).

values presented in all tables to present differences in scaling law prediction, these values have been calculated according to deviation of bigger specimen ($n = 1$) from smaller specimen ($n = 1/2$). This table illustrates that mechanical properties of two scaled sizes are close together approximately, and maximum difference in scaling law prediction is 9% which corresponds to maximum strain. As a result, FMLs obey scaling law under tensile loading experimentally.

In order to investigate the scaling law in numerical study, the first step is to ensure accuracy of numerical results, so for example, the numerical and experimental results which were obtained for smaller sample ($n = 1/2$) were compared with each other as shown in Figure 5.

Figure 5 shows that there is a good agreement between the numerical and experimental results. Through a closer investigation of Figure 5, it can be concluded that the two curves are close together until line A. Deviation between curves begins from line A and continues to line B where at this line (0.1% strain), the two curves have the same value. Differences between curves from line A to B are due to the fact that debonding between aluminum and composite layers gradually happens in the experiment, whereas in numerical simulation debonding occurs suddenly before line B, and from line A to B the linear response is seen. After line B, composite and aluminum layers are under tensile loading separately and so the two curves have linear behavior until final failure (line C).

Ultimate stress and maximum strain which are predicted by numerical simulation are close to experimental data as presented in Table 4. According to Figure 5 and Table 4, numerical simulation can be used to evaluate scaling law.

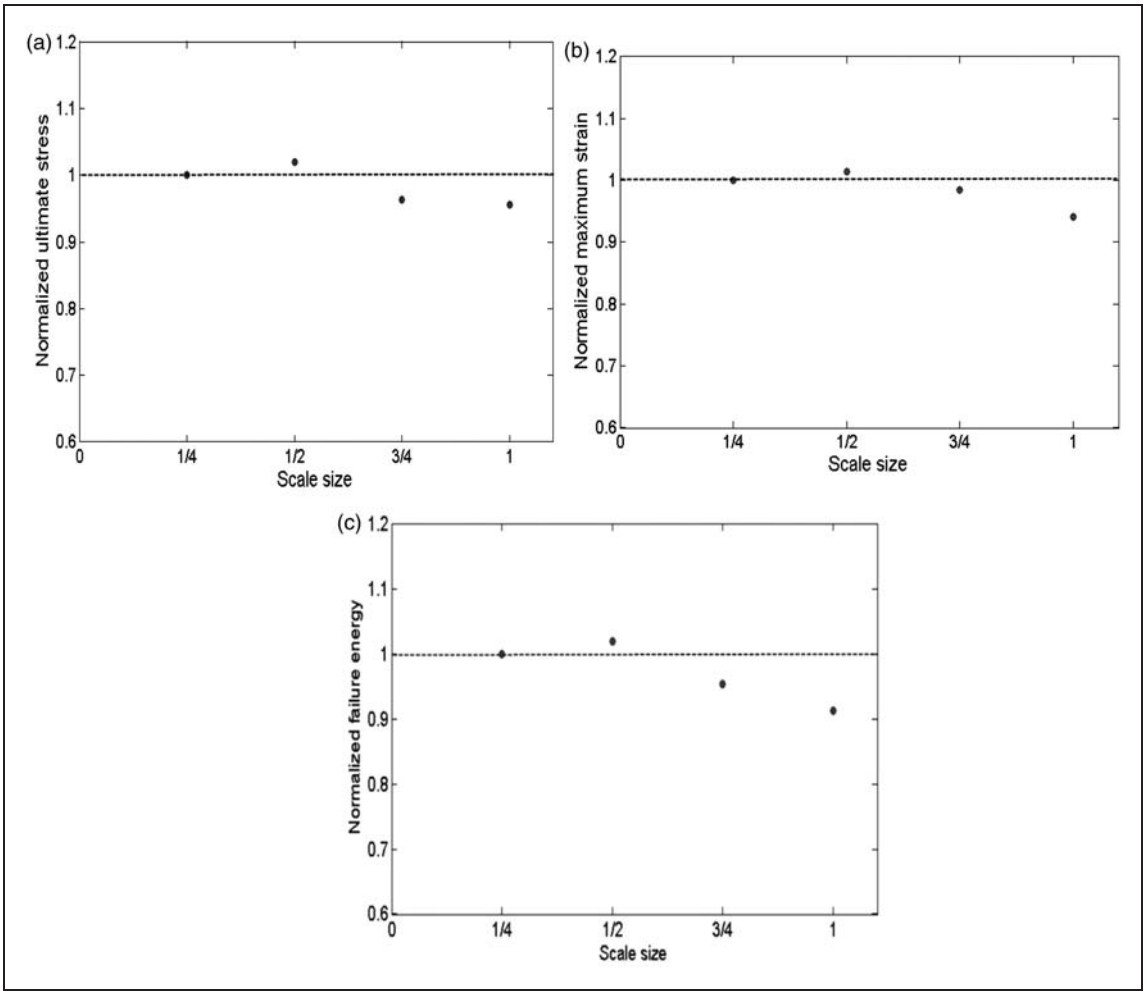

Figure 7. Normalized parameters of four scaled sizes of FMLs under tensile loading (numerical study). (a) Normalized ultimate stress, (b) normalized maximum strain, and (c) normalized failure energy.

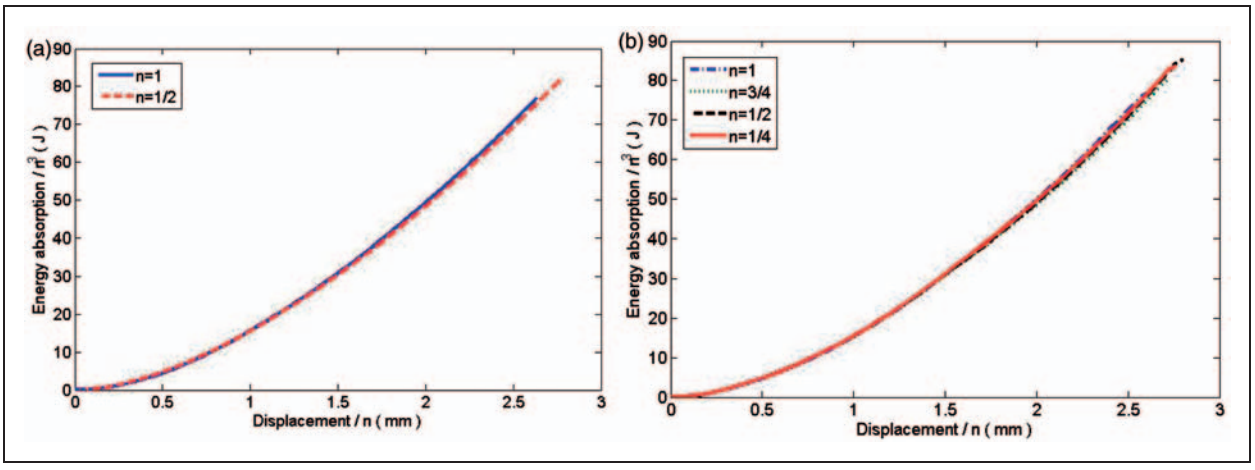

Figure 8. Comparison of normalized experimental energy–displacement curves for different scaled sizes of FMLs under tensile loading.

In order to investigate scaling rule numerically, normalized parameters such as ultimate stress, maximum strain, and failure energy should be discussed. The stress–strain curves which were obtained numerically are plotted in Figure 6 and the detailed results of them are presented in Figure 7. Figure 6 shows that four curves are the same before debonding between metal and composite layers, but after debonding, curves deviate from each other. So, scaling law is exactly validated for FMLs in numerical study

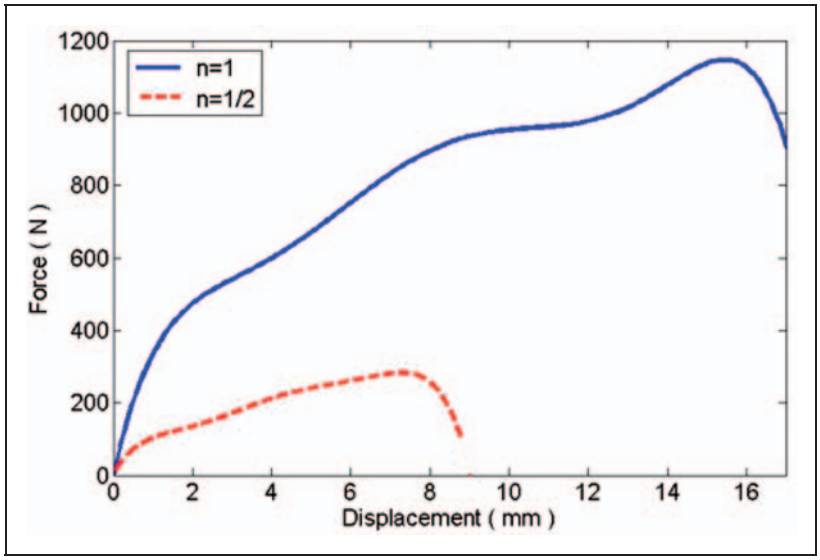

Figure 9. Comparison of experimental force–displacement curves for two scaled sizes of FMLs under three-point bending.

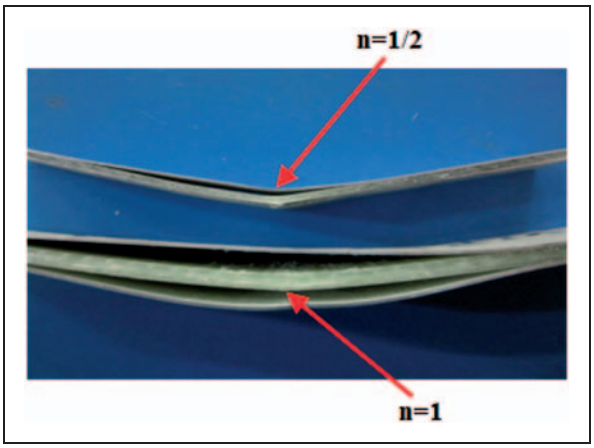

Figure 10. Debonding between aluminum and composite layers after three-point bending test.

before debonding while it cannot be seen after debonding part. Therefore, some normalized parameters should be investigated such as normalized ultimate stress, maximum strain, and failure energy which are depicted in Figure 7. According to this figure, maximum difference is seen in normalized failure energy between all normalized parameters. This difference is 8.9% for numerical process. Consequently, responses of scaled sizes of FMLs keep to scaling law under tension.

Because maximum difference in scaling law prediction was failure energy in numerical process, it is needed to find out the accuracy of scaling law prediction for energy absorption at each displacement. So, normalized energy–displacement curves are plotted in Figure 8. This figure shows that normalized energy absorption of different scaled sizes is close together at each displacement before final failure. Also, difference between normalized failure energy of different scaled sizes is due to differences between normalized ultimate stress and maximum strain.

Three-point bending results

In this part of the study, different scaled sizes of FMLs were investigated under three-point bending test. Force–displacement curves obtained from experiments are plotted in Figure 9. According to this figure, both scaled sizes have similar responses under three-point bending that includes elastic, plastic, and rupture parts. The inspection of samples introduces that failure modes are the same in all of them. The main failure is debonding between metal and composite layers as shown in Figure 10. This failure occurs by shear forces between layers. Also in bigger specimen, debonding occurs between two metal layers and composite layers, while debonding occurs between upper metal layer and composite layer in smaller specimen. Delamination between composite layers is another failure mode which is seen in the cases. Fiber breakage did not happen in these tests, whereas this failure mode occurred in tensile test.

In order to show the compatibility between the numerical and experimental results, force–displacement curves of them are presented in Figure 11 for smaller specimen ($n = 1/2$). This figure demonstrates that numerical simulation can predict the behavior of FMLs under bending with good accuracy. Table 5 presents that maximum force and displacement are close together in numerical and experimental study and have differences of 13.8 and 3.3%, respectively. According to Figure 11 it can be seen that for points between line A and B, the difference between numerical simulation and experiment is considerable. This difference is due to the fact that debonding between aluminum and composite layers gradually happens in

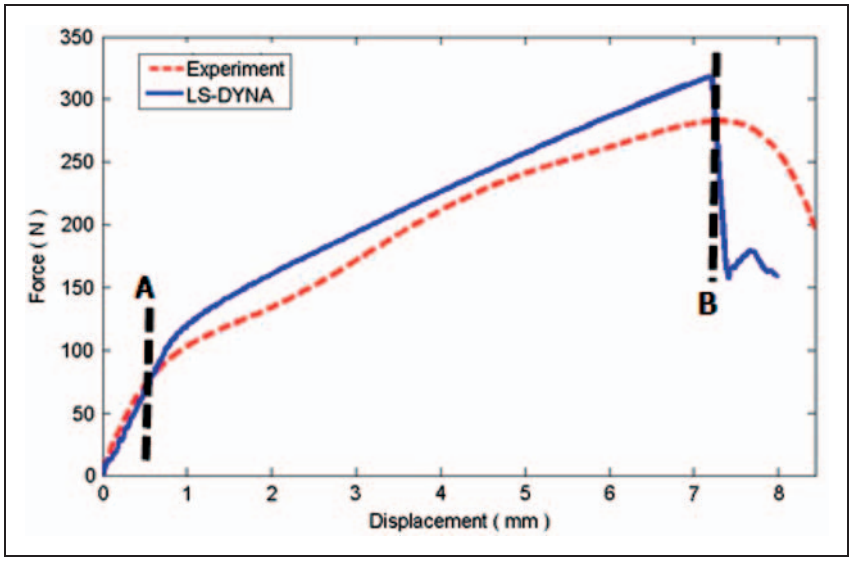

Figure 11. Comparison of numerical and experimental force–displacement curves for FML under three-point bending.

Table 5. Experimental and numerical three-point bending results for smaller FML specimen.

	Experimental	Numerical	Error (%)
Maximum load (N)	282 ($_{\downarrow}-^{\uparrow}+$)2.5)	321.2	13.8
Maximum displacement (mm)	7.44 ($_{\downarrow}-^{\uparrow}+$)0.08)	7.2	3.3

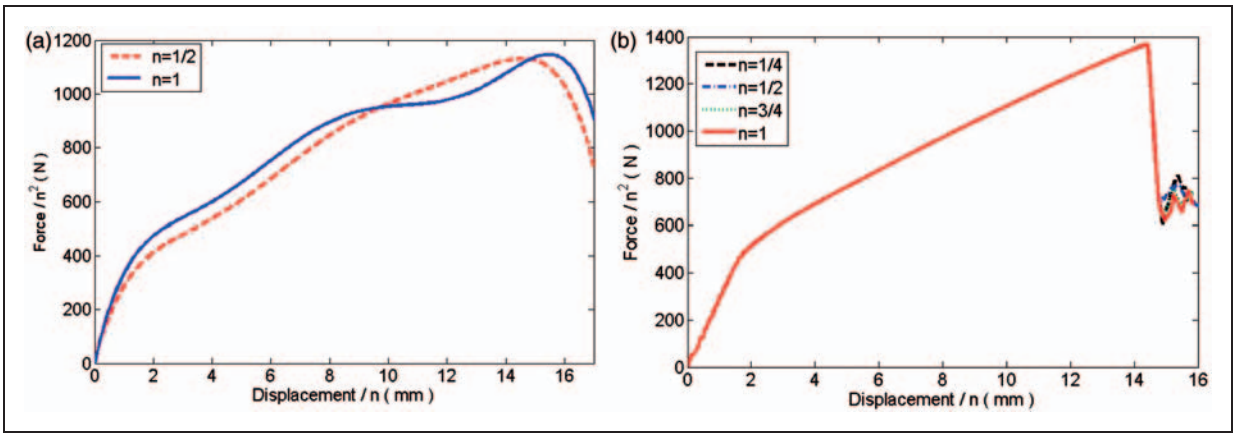

Figure 12. Comparison of normalized force–displacement curves for different scaled sizes of FMLs. (a) Experiment, (b) numerical simulation.

the experiment, whereas in numerical simulation, debonding occurs suddenly at line B.

In order to show the numerical and experimental validation of scaling law for FMLs under three-point bending, normalized force–displacement curves are illustrated in Figure 12. According to this figure, the normalized force–displacement curves for different sizes are the same approximately. In numerical process, four curves are exactly the same (see Figure 12(b)). Numerical simulation in tensile modeling showed that scaling law is exactly valid before first failure mode that was debonding. Since debonding is seen in three-point bending modeling as the first and final failure mode, it can be concluded that in numerical study, scaling rule is exactly valid for FMLs under bending until final failure. Also Figure 12(a) shows that scaling law has a little difference in experimental study. In order to find the value of these differences, normalized maximum force, maximum displacement, and failure energy are tabulated in Table 6. This table explains that maximum difference is 10.3% that refers to failure energy. Therefore, FMLs obey scaling laws under bending with good accuracy.

Table 6. Normalized parameters of two scaled sizes of FMLs under three-point bending test.

	$n = 1/2$	$n = 1$	Difference (%)
Maximum force/n^2 (N)	1119($_{\downarrow}$ $-^{\uparrow}$ +)10)	1153($_{\downarrow}$ $-^{\uparrow}$ +)16)	3
Maximum displacement/n (mm)	14.42($_{\downarrow}$ $-^{\uparrow}$ +)0.16)	15.61($_{\downarrow}$ $-^{\uparrow}$ +)0.12)	8.2
Failure energy/n^3 (J)	11.20($_{\downarrow}$ $-^{\uparrow}$ +)0.10)	12.36($_{\downarrow}$ $-^{\uparrow}$ +)0.14)	10.3

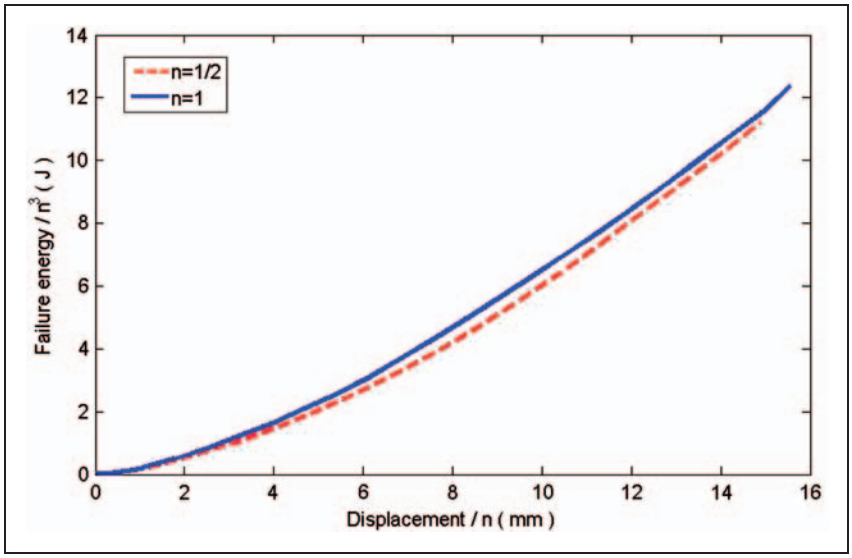

Figure 13. Comparison of normalized energy–displacement curves for two scaled sizes of FMLs.

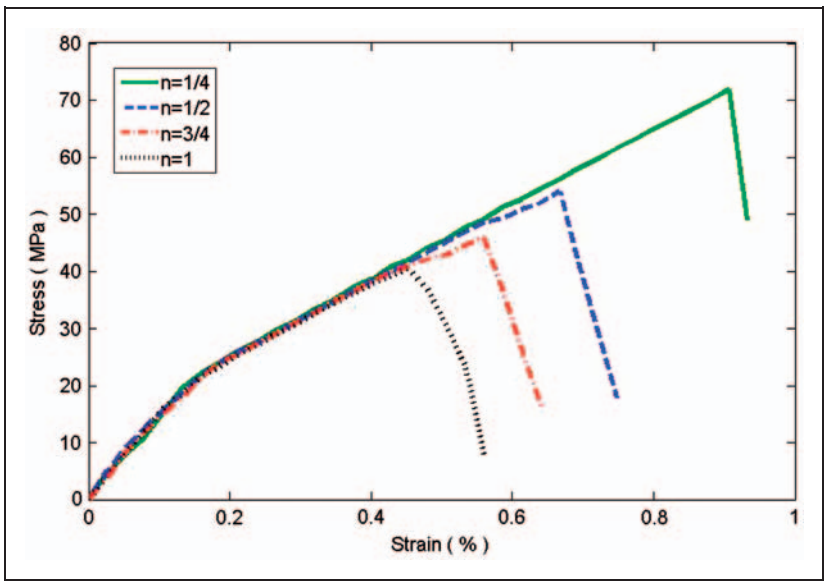

Figure 14. Comparison of stress–strain curves for four scaled sizes of FMLs with open hole (numerical results).

Absorbed energy at each displacement is another parameter that can be checked to investigate the scaling rule. Figure 13 shows energy absorption–displacement curves were obtained experimentally for two scaled sizes of FMLs under three-point bending. The two curves deviate from each other by approaching the rupture point according to Figure 13.

Open hole specimen under tensile loading

FMLs used in industries in most cases have a circular cutout because they are usually connected to the other parts by bolt or rivet joints. Therefore, investigating scaling law in FMLs with hole is very important. In this part, the specimen with a circle hole is investigated numerically. The ratio of hole diameter to width

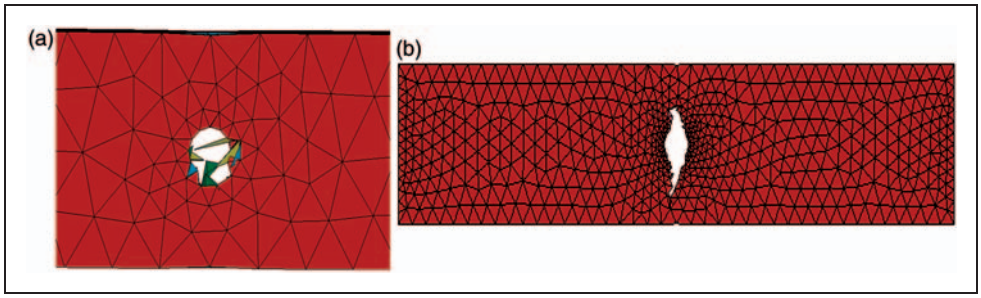

Figure 15. Failure mode in open hole specimen. (a) Smaller specimen, and (b) bigger specimen.

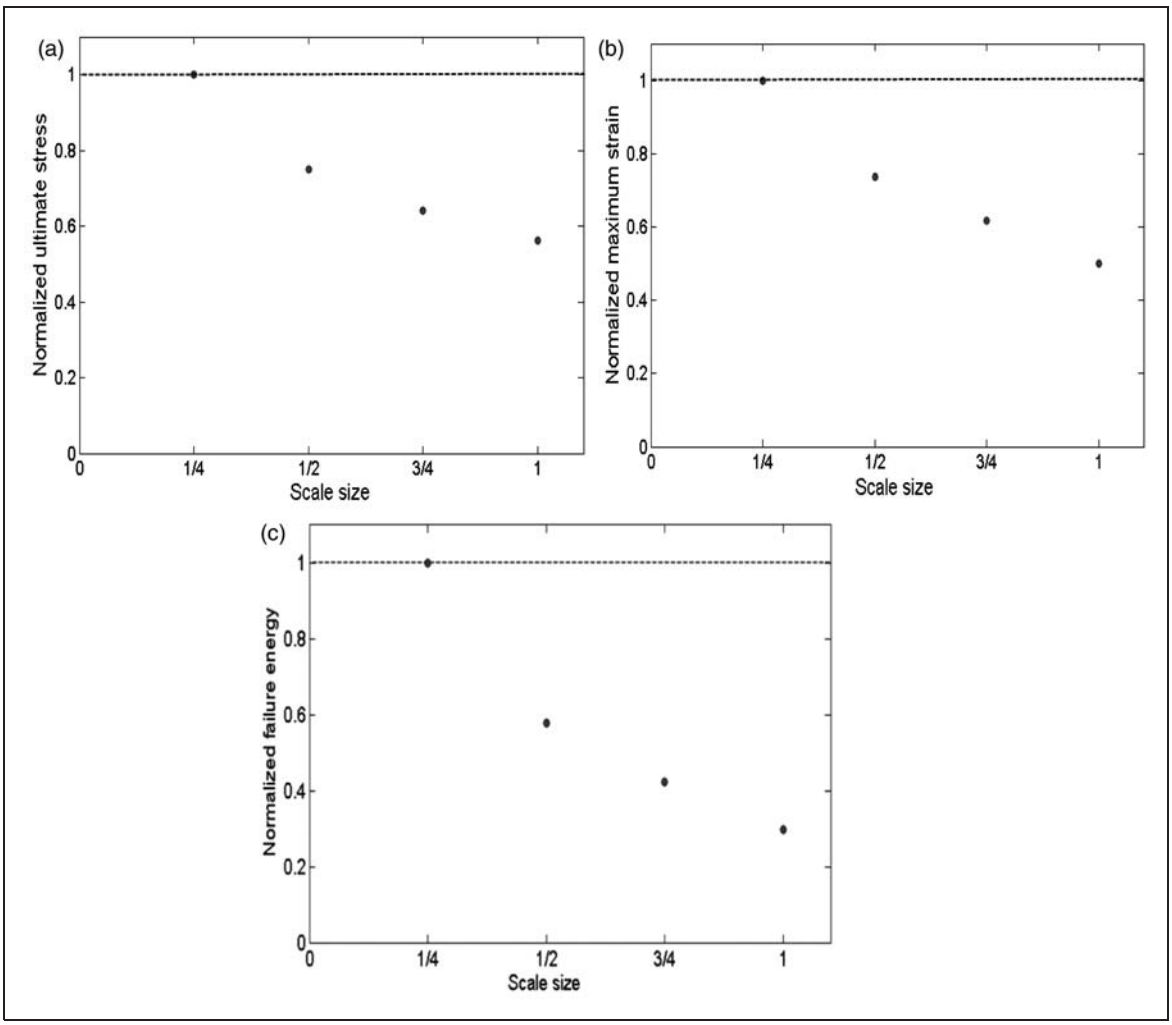

Figure 16. Normalized parameters of four scaled sizes of FMLs with open hole under tensile loading (numerical study). (a) Normalized ultimate stress, (b) normalized maximum strain, and (c) normalized failure energy.

of samples is 0.2 and all dimensions are similar to dimensions in Figure 1. Stress–strain curves for four scaled sizes of FMLs were presented in Figure 14. Comparison of each two curves of four curves shows that they are very close together until rupture point of bigger case. The difference between ultimate stresses of them is due to the existence of hole in samples. Although the ratio of hole diameter to width of samples is the same, the stress intensity factor rises by increase in specimen's size because the stress intensity factor for a circular hole has theoretically a direction relationship with the radius of the hole.[29] That means if the radius of a hole increases, the stress intensity factor increases too. As a result, the bigger specimen has higher stress intensity factor than smaller specimen, which causes the ultimate stress to decrease and the structure to have more brittle response by specimen's becoming bigger. This hole causes a change in

failure modes as shown in Figure 15. As shown in Figure 15(b), in the biggest specimen, aluminum tearing and fiber fracture occur at 90° to the load direction. On the other hand, in the smaller specimens, the failure modes are the combination of pull out and debonding. Consequently, specimen has the brittle response in bigger specimen due to the higher value of stress intensity factor, and ultimate stress decreases. This result tallies with Refs. 20–23. Normalized parameters such as ultimate stress, maximum strain, and failure energy for four scaled sizes of FMLs with open hole are shown in Figure 16. This figure demonstrates that hole size effect is strong in FML specimens. The maximum deviation is 44, 50, and 70% in normalized ultimate stress, maximum strain, and failure energy, respectively.

Conclusion

Scaling effect on FMLs under tensile loading and three-point bending has been investigated numerically and experimentally. In tensile loading, two scaled sizes of samples have similar behavior and failure modes that included fiber breakage, delamination between composite layers, debonding between metal and composite layers, and aluminum fracture in both cases. Also mechanical properties such as elastic modulus, maximum strain, yield, and ultimate stress of two specimens are close together approximately. In three-point bending test, two scaled sizes of FML have the same behavior. Debonding between aluminum and composite layers and delamination between composite layers were seen in both cases. Numerical simulation can predict the behavior of FMLs under tensile loading and three-point bending with good accuracy. Scaling law is exactly valid for four scaled sizes of FML before first failure mode in numerical process and after failure, there is difference in scaling rule prediction. Also, numerical simulation demonstrates that hole size effect is considerable in FML specimens. Hole size effect led to this observation that by increasing the size of the sample, the failure mode changes and ultimate stress decreases. The effect of considering the interface in numerical modeling by using cohesive zone elements or modeling the resin layers on the validation of scaling law could be investigated in the future studies.

Funding

This research received no specific grant from any funding agency in the public, commercial, or not-for-profit sectors.

References

1. A Vlot and JW Gunnink (eds) *Fiber metal laminates—an introduction*. Dordrecht: Kluwer Academic Publisher, 2001.
2. Vlot A. *Glare*. Dordrecht: Kluwer Academic Publisher, 2001.
3. Sadighi M, Alderliesten RC and Benedictus R. Impact resistance of fiber-metal laminates: A review. *Int J Impact Eng* 2012; 49: 77–90.
4. Morton J. Scaling of impact-loaded carbon-fiber composites. *AIAA J* 1988; 26(8): 989–994.
5. Sutherland LS and Guedes Soares C. Scaling of impact on low fibre-volume glass–polyester laminates. *J Compos Part A* 2007; 38: 307–317.
6. Viot P, Ballere L, Guillaumat L, et al. Scale effects on the response of composite structures under impact loading. *J Fract Mech* 2008; 75: 2725–2736.
7. Christoforou AP and Yigit AS. Scaling of low velocity impact response in composites structures. *J Compos Struct* 2009; 91: 358–365.
8. Qian Y, Swanson SR, Nuismer RJ, et al. An experimental study of scaling rules for impact damage in fiber composites. *J Compos Mater* 1990; 24(5): 559–570.
9. Swanson SR. Scaling of impact damage in fiber composites from laboratory specimens to structures. *J Compos Struct* 1993; 25: 249–255.
10. Jackson KE, Kellas S and Morton J. Scale effects in the response and failure of fiber reinforced composite laminates loaded in tension and in flexure. *J Compos Mater* 1992; 26(18): 2674–2705.
11. Kellas S and Morton J. Strength scaling in fiber composites. NASA CR 4335, 1995.
12. Wisnom MR. The effect of specimen size on the bending strength of unidirectional carbon fiber-epoxy. *J Compos Struct* 1991; 18(1): 47–63.
13. Carrillo JG and Cantwell WJ. Scaling effects in the tensile behavior of fiber-metal laminates. *Compos Sci Technol* 2007; 67: 1684–1693.
14. Carrillo JG and Cantwell WJ. Scaling effects in the low velocity impact response of fiber–metal laminates. *J Reinf Plast Compos* 2008; 27(9): 893–907.
15. McKown S, Cantwell WJ and Jones N. Investigation of scaling effects in fiber–metal laminates. *J Compos Mater* 2008; 42: 865–888.
16. Awerbuch J and Madhukar MS. Notched strength of composite laminates: Predictions and experiments—a review. *J Reinf Plast Compos* 1985; 4: 153–159.
17. Eriksson I and Aronsson CG. Strength of tensile loaded graphite/epoxy laminates containing cracks, open and filled holes. *J Compos Mater* 1990; 24: 456–482.
18. Chang KY, Liu S and Chang FK. Damage tolerance of laminated composites containing an open hole and subjected to tensile loadings. *J Compos Mater* 1991; 25: 274–301.
19. De Morais AB. Open-hole tensile strength of quasi-isotropic laminates. *Compos Sci Technol* 2000; 40: 1997–2004.
20. Winsom MR and Hallett SR. Scaling effects in notched composites. *J Compos Mater* 2010; 44: 195–210.
21. Green BG, Winsom MR and Hallett SR. An experimental investigation into the tensile strength scaling of notched composites. *J Compos Part A: Applied Sci Manuf* 2007; 38: 867–878.
22. Hallett SR, Green BG, Jiang WG, et al. An experimental and numerical investigation into the damage mechanisms in notched composites. *J Compos Part A: Appl Sci Manuf* 2009; 40: 613–624.
23. Winsom MR and Hallett SR. The role of delamination in strength, failure mechanism and hole size effect in

open hole tensile tests on quasi-isotropic laminates. *J Compos Part A: Appl Sci Manuf* 2009; 40: 335–342.
24. Iaccarino P, Langella A and Caprino G. A simplified model to predict the tensile and shear stress-strain behaviour of fibreglass/aluminium laminates. *Compos Sci Technol* 2007; 67(9): 1784–1793.
25. LS-DYNA keyword user's manual, V971, LSTC. Livermore Software Technology Corporation, May 2007.
26. Sadighi M, Parnanen T, Alderliesten RC, et al. Experimental and numerical investigation of metal type and thickness effects on the impact resistance of fiber metal laminates. *Appl Compos Mater* 2012; 19: 545–559.
27. Menna C, Asprone D, Caprino G, et al. Numerical simulation of impact tests on GFRP composite laminates. *Int J Impact Eng* 2011; 38: 677–685.
28. Haghi Kashani M, Shahsavari Alavijeh H, Akbarshahi H, et al. Bitubular square tubes with different arrangements under quasi-static axial compression loading. *J Mater Des* 2013; 51: 1095–1103.
29. Kamala Kannan V, Murali V, Rajadurai A, et al. Tension and compression strength evaluation of composite plates with circular holes. *J Reinf Plast Compos* 2010; 29: 1500–1514.